1 **Effects of Estrogen-Deficient State on Rotator Cuff Healing**

2

3

4

5

6 Koji Tanaka, MD, Tomonoshin Kanazawa, MD, PhD, Masafumi Gotoh, MD,
7 PhD, Ryo Tanesue, MD, PhD, Hidehiro Nakamura,MD, PhD, Hiroki Ohzono,
8 MD, PhD, Takahiro Okawa, MD, PhD, and Naoto Shiba, MD, PhD

9
10 *Investigation performed at the Kurume University School of Medicine, Kurume,*
11 *Japan, and Kurume University Medical Center, Kurume, Japan*

12

13

14   **Abstract**

15   **Background:** Rotator cuff retears after surgical repair are of concern despite advances in

16   operative techniques, but few studies have investigated the effects of estrogen-deficiency

17   state on tendon-to-bone healing at the repair site.

18   **Purpose:** We evaluated the effect of estrogen-deficiency state on tendon-to-bone healing

19   after rotator cuff repair in an ovariectomized rat model.

20   **Study Design:** Controlled laboratory study

21   **Methods:** Female Sprague–Dawley rats underwent detachment and immediate repair of the

22   supraspinatus tendon. Surgery was performed in 24 rats 17 weeks after ovariectomy (OVX

23   group) and in 24 age-matched control rats without ovariectomy. Animals were sacrificed at 2,

24   4, 8, and 12 weeks after surgery for biomechanical and histological evaluation of reattachment.

25   Bone mineral density (BMD) at the insertion site and cancellous bone in the humeral head was

26   assessed by microcomputed tomography.

27   **Results:** BMD was significantly lower at both the insertion site and cancellous area in OVX

28   than in control rats at weeks 2–12. Ultimate load to failure, ultimate stress, stiffness, and

29   Young's modulus were significantly lower in the OVX than in the control group at 2 and 4

30   weeks, but the difference was no longer significant at 8 and 12 weeks. At 2 and 4 weeks,

31   relatively immature granulation tissue was observed in OVX rats compared with control rats.

32   At 8 and 12 weeks after surgery, there were differences in the tendon–bone interface in the

33   two groups: Direct insertion with well-established chondroid tissue was seen in the control

34   group. Indirect insertion without chondroid tissue was seen in the OVX group. Consistently,

35   the amount of chondroid tissue was greater, and collagen organization was better in the

36   control than in the OVX rats. Cells expressing cathepsin K were significantly more numerous

37   at both the insertion site and in the cancellous bone in OVX rats than in control rats.

Conclusion: Estrogen-deficiency state by ovariectomy, compared with control rats, led to decreased biomechanical properties and development of chondroid tissue that influenced the repair of tendon insertion following surgery.

Clinical Relevance: Agents that modulate bone metabolism might improve tendon-to-bone healing in patients with estrogen-deficiency state, such as postmenopausal women who experience rotator cuff surgery.

Key Terms: bone mineral density, biomechanics, tendon-to-bone healing, rotator cuff tear

What is known about the subject: Rotator cuff repairs have good outcomes, but postoperative retears are a concern. Age, tear size, fatty infiltration of rotator cuff muscles, and surgical variables have been shown to influence the risk of retears. The effects of estrogen-deficiency state on tendon-to-bone healing after cuff repair are not known.

What this study adds to existing knowledge: This study investigated the effects of estrogen-deficiency state on tendon-to-bone healing in a rotator cuff repair model in ovariectomized (OVX) rats. Mechanical properties including ultimate load to failure, ultimate stress, linear stiffness, and Young's modulus were significantly lower in the OVX than in the control rats at 2 and 4 weeks after surgery. The differences were no longer significant at 8 and 12 weeks. Histological differences at 2 and 4 weeks after surgery included relatively immature granulation tissue in the OVX compared with control rats. At 8 and 12 weeks, there were differences in the tendon–bone interface. Direct insertion with well-established chondroid tissue was seen in control rats. Indirect insertion without chondroid tissue was seen in OVX rats. Safranin O staining was more extensive in control than in OVX group tissues. Picrosirius red staining indicated better collagen organization in the control group than in the OVX rats. The number of cathepsin K-stained cells was significantly higher in OVX rats than in control rats at both the tendon insertion site and in cancellous bone from 4 to 12 weeks after tendon reattachment. The results are consistent with the association of estrogen-

64   deficiency state in OVX rats with decreased biomechanical strength and of chondroid tissue

65   development that altered rotator cuff reinsertion and healing after surgery.

66

INTRODUCTION

Surgical repair, the primary treatment for rotator cuff tears, has a reported failure rate of from 5% to 57%.[2,8,9,32,39] Retear rates of 5% have been reported for small-to-medium tears and 40% for large, extensive tears.[36]

 A better understanding of tendon-to-bone healing after rotator cuff repair would help to find ways of reducing the occurrence of retears. Tendon–bone insertions include four zones that include tendon, fibrocartilage, mineralized cartilage, and bone[2,8] act to transfer stress between dissimilar materials. The transition from mineralized cartilage to tendon is continuous, and there are no clearly defined boundaries between the zones, even on an ultrastructural level.[20] The insertion acts as a shock absorber to reduce the stiffness gradient between bone and tendon.[26] The histological and biomechanical characteristics of the tendon–bone interface following surgical repair differs from normal tendon insertions, resulting in a tendon–bone interface weaker than that of normal tendon insertions.[32,37] Mineralized bone activity also influences tendon-to-bone healing after cuff repair.[6,14,24,33] Both BMD and fatty infiltration were found to be independently associated with postoperative rotator cuff healing[6,11]. Thus, these results suggest that estrogen deficiency causing low mineralized bone activity may influence tendon bone healing after surgery. Therefore, this study evaluated the effects of estrogen deficiency on tendon-to-bone healing after cuff repair in an ovariectomized rat model.

MATERIAL AND METHODS

Study design

The study was conducted following the National Institute of Health Guidelines for Animal Research and approved by the Animal Studies and the Institutional Animal Care and Use Committees of our institution (# 2018-083). Forty-eight adult female Sprague–Dawley rats weighing 415.5 ± 26.5 g underwent ovariectomy followed by detachment and immediate

93   repair of the supraspinatus tendon at 17 weeks of age (OVX group, $N = 24$). The remaining

94   24 age-matched, nonovariectomized rats were used as a control group. The repaired tendon-

95   to-bone interface was evaluated in both groups at 2, 4, 8, and 12 weeks after surgery (Figure

96   1). Bone mineral density (BMD) was assessed by microcomputed tomography (micro-CT).

97   Biomechanical properties, tissue histology, immunohistochemical staining, and osteoclast

98   activity at the attachment site were assessed as described below.
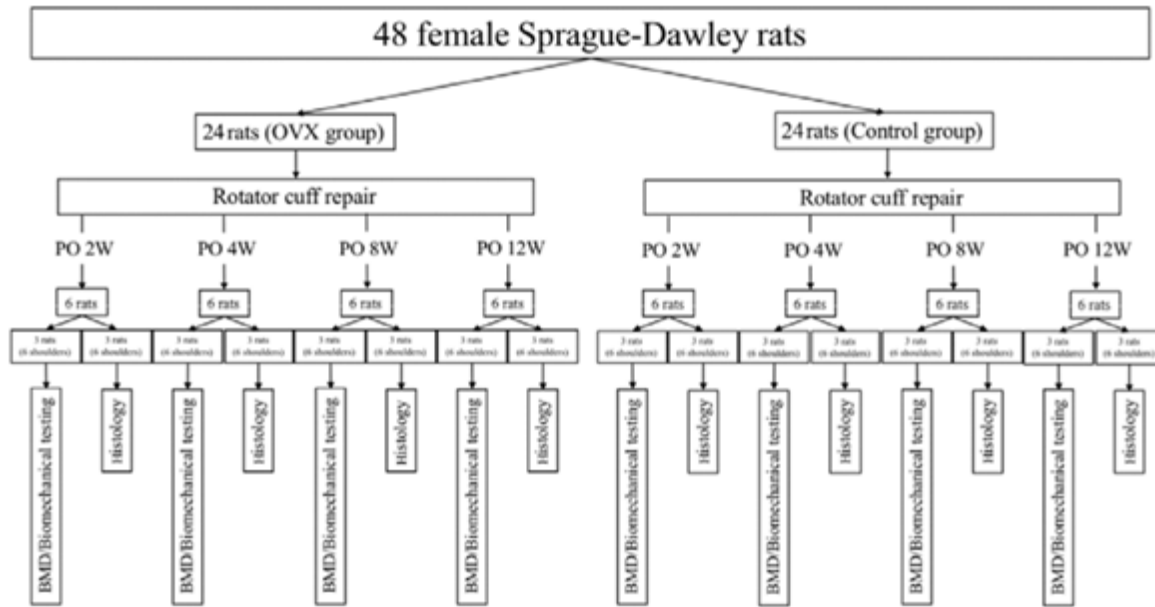
99

100   Figure1. Flow diagram of the study design indicating the group allocations and study

101   procedures.

102

103   **Rotator cuff repair model**

104   The surgical procedure was performed as previously described.[19] Briefly, rats were anesthetized

105   with isoflurane with high flow oxygen. A midline skin incision was made, the subcutaneous tissues

106   were divided, and the deltoid muscle was divided to expose the shoulder joint. The supraspinatus

107   tendon insertion was excised at its attachment to the humerus with a #11 scalpel blade. The

108   remaining tendon tissue was removed, and two small tunnels were created at the greater tuberosity

109   with a 0.5 mm drill bit. Sutures were passed through the supraspinatus tendon using the Krakow

110   technique, pulled through the bone tunnels, and firmly tied to the lateral cortex. After wound

111   closure, animals could move freely in their cages.

112

113   **BMD and bone volume assays**

114   BMD was determined at the tendon attachment site and in cancellous bone in the head of the

115   humerus by micro-CT (R-mCT2, Rigaku Corporation, Japan). Six specimens were collected at each

116   designated time following sacrifice and immediately frozen at −80 °C until tested. To collect the

117   specimens, all soft tissue surrounding the humerus was removed except for the repaired

118   supraspinatus tendon–humerus complex. The sutures that had been used to fix the repaired tendon

119   to the bone were cut, and the repaired tendon was secured in a screw clamp using sandpaper and

120   ethyl cyanoacrylate. Micro-CT was performed with the specimens submerged in saline and scanned

121   at 90 kV and 160 μA. The images were analyzed with BMD analysis software (TRI/3D-BON,

122   Ratoc System Engineering Co., Japan); phantom images of a bone reference material were used for

123   calibration.[30] The image threshold at the tendon attachment site was 5 mm from the proximal end of

124   the humeral head. In cancellous bone, the image threshold was within the bone cortex, 6 mm from

125   the proximal end of the humeral head. The bone volume (BV) was the total number of thresholded

126   bone voxels within the total volume (TV) of the volume of interest (VOI). After thresholding, the

127   total bone mineral content, BV fraction (BV/TV), and BMD were calculated for the VOI at both the

128   supraspinatus tendon attachment site and in the cancellous bone. For BMD analysis, the threshold

129   was 300 Hounsfield units.

130

131   **Biomechanical testing**

132   Biomechanical testing was done immediately following micro-CT scanning. Specimens were

133   placed into a tensile strength testing device (TENSILON RTE-1210; Orientec, A&D Company,

134   Limited, Tokyo, Japan), and the humerus was secured in a custom-designed pod using a capping

135   compound.[17,19,28] The testing protocol, with some modifications, has been previously

136   described.[11,15,16,19] The tendon–humerus complex was positioned to allow longitudinal tensile

137   loading in the direction of tendon attachment site. Specimens were preloaded at 0.1 N for 5 minutes,

138   followed by five cycles of loading and unloading at a cross-head speed of 5 mm/ minutes. They

139   were then loaded to failure at a rate of 1 mm/ minutes. The mechanical properties were calculated,

140   and the failure modes were recorded. Ultimate load to failure was recorded as the peak load before

141   failure. Linear stiffness was determined by the slope of the linear portion of the load-elongation

142   curve. Ultimate stress was calculated by dividing the ultimate load to failure by the cross-sectional

143   area of the repaired tendon–bone interface, the axial section of the micro-CT image. Young's

144   modulus was calculated from the slope of the linear portion of the stress–strain curve. Strain was

145   calculated by dividing the elongation by the initial length of the coronal section of the micro-CT

146   image.

147

148   **Histological evaluation**

149   Supraspinatus tendon–humerus specimens were fixed in 10% buffered formalin, decalcified with

150   Kalkitox solution (Wako Pure Chemical Industries, Ltd., Osaka, Japan), embedded in paraffin, and

151   sectioned at 5 μm.[21] After staining with hematoxylin and eosin (HE), safranin O, or picrosirius red,

152   the sections were observed by light (BZ-X710; Keyence, Osaka, Japan) and a polarized light

153   microscopy (OLYMPUS BX50; OLYMPUS, Tokyo, Japan) and photographed.[22]

154

155   **Immunohistology**

156   Immunostaining was performed with polyclonal antibodies against cathepsin K (Abcam, Tokyo,

157   Japan) using the Envision method (Agilent, Santa Clara, CA, United States). After deparaffinization

158   of the tissue sections, antigen activation was performed in 3% bovine serum albumin for 30 minutes

159   at room temperature. Blocking of endogenous peroxidase was by incubation with methanol

160   containing 3% H_2O_2 for 30 minutes at room temperature. The primary antibody was diluted to an

161   appropriate concentration with Anti-Diluent Buffer, and each reaction was performed overnight at

162   4 °C. Polyclonal anti-rabbit immunoglobulin conjugated to peroxidase labeled dextran polymer was

163   used as the secondary antibody (DAKO, K4001) and was allowed to react for 30 minutes at room

164   temperature. Diaminobenzidine was used as a chromogen. The sections were counterstained with

165   hematoxylin and observed by light microscopy (BZ-X710; Keyence, Osaka, Japan).

166

167   **Histomorphology**

168   Osteoclast activity was assayed by cathepsin K immunohistochemical staining and tendon–bone

169   maturity by semiquantitative scoring as previously described.[25,35.] At 2, 4, 8, and 12 weeks, three

170   slides of sectioned tissue from each specimen were randomly selected for analysis.

171   Photomicrographs were taken of five ×100 fields on each slide. A total of 240 photomicrographs,

172   60 each week including 30 OVX group specimens and 30 control group specimens, were collected

173   and evaluated. The cathepsin K-positive cells on each slide were automatically counted using

174   ImageJ macro software (U. S. National Institutes of Health, Bethesda, Maryland, USA)

175   (https://imagej.nih.gov/ij/docs/index.html).

176

177   **Statistical analysis**

178   Statistical analysis was performed with JMP version 13 (SAS Institute Inc., Cary, NC, USA). Data

179   were expressed as means and standard deviation. Differences of BMD, mechanical properties, and

180   histomorphometric scores in the OVX and control groups were tested for significance with the

181   Wilcoxon test. $P < 0.05$ was considered significant.

182

183   **RESULTS**

184

185   **BMD**

186   The areas in which BMD was measured are shown in Figure 2A. The BMD in cancellous bone

187   599.45 ± 92.83 mg/cm^3 in controls and 374.68 ± 23.35 mg/cm^3 in OVX rats at 2 weeks, $667.97 \pm$

188 84.76 and 438.94 ± 74.23 mg/cm^3 at 4 weeks, 710.28 ± 138.28 and 493.12 ± 123.03 mg/cm^3 at 8

189 weeks, and 735.68 ± 57.89 and 461.17 ± 55.76 mg/cm^3 at 12 weeks. At each time, the BMD of

190 cancellous bone was significantly lower in the OVX group than in controls (Figure 2B). The

191 corresponding BMD in the insertion area was 667.4 ± 39.75 and 581.83 ± 15.54 mg/cm^3 at 2 weeks,

192 639.73 ± 16.1 and 578.85 ± 29.54 mg/cm^3 at 4 weeks, 761.73 ± 22.87 and 700.57 ± 39.9 mg/cm^3 at

193 8 weeks, and 809.55 ± 64.94 and 639.73 ± 53.91 mg/cm^3 at 12 weeks. At each time, the BMD of

194 cancellous bone was significantly lower in the OVX group than in controls (Figure 2C).

195

196

197 Figure 2. (A) Histology of the supraspinatus tendon insertion in ovariectomized and control rats.

198 The boxes indicate the insertion site and cancellous bone in the humeral head. The mineral density

199 of the (B) cancellous bone of the humerus and (C) the tendon insertion site are shown.

200

201 **Biomechanical testing**

202 Tendon attachment failed during biomechanical testing in all specimens of both experimental

203 groups. The ultimate load to failure was 9.15 ± 4.34 and 4.22 ± 1.06 N in the control and

204 OVX groups, respectively, at 2 weeks, 20.94 ± 4.01 and 16.62 ± 5.53 N at 4 weeks, 28.58 ±

205   9.54 and 23.98 ± 7.29 N at 8 weeks, and 33.87 ± 9.77 and 28.09 ± 6.73 N at 12 weeks. The

206   load was significantly lower in the OVX than in the control group at 2 and 4 weeks, but the

207   difference was no longer significant at 8 and 12 weeks (Figure 3A). Linear stiffness was 6.8 ±

208   1.27 N/mm in the OVX and 3.59 ± 0.98 N/mm in the control group at 2 weeks, 8.97 ± 2.41

209   and 7.04 ± 4.76 N/mm at 4 weeks, 15.23 ± 3.57 and 14.54 ± 5.84 N/mm at 8 weeks, and

210   17.33 ± 4.51 and 16.01 ± 3.15 N/mm) at 12 weeks. Linear stiffness was significantly lower in

211   the OVX than in the control group at 2 and 4 weeks, but the difference was no longer

212   significant at 8 and 12 weeks (Figure 3B). Ultimate stress values were 0.87 ± 0.49 MPa in the

213   control and 0.34 ± 0.15 MPa in the OVX group at 2 weeks, 1.18 ± 0.42 and 0.72 ± 0.26 MPa

214   at 4 weeks, 1.74 ± 0.76 and 1.4 ± 0.74 MPa at 8 weeks, and 1.77 ± 0.68 and 1.57 ± 0.62 MPa

215   at 12 weeks. Ultimate stress was significantly lower in the OVX group than in the control

216   group at 2 and 4 weeks, but the difference was no longer significant at 8 and 12 weeks

217   (Figure 3C). Young's modulus was 1.46 ± 0.34 MPa in the OVX group and 0.56 ± 0.22 MPa

218   in the control group at 2 weeks, 1.66 ± 0.81 and 1.34 ± 0.73 MPa at 4 weeks, 2.88 ± 2.0 and

219   2.8 ± 1.46 MPa at 8 weeks, and 3.16 ± 1.97 and 2.98 ± 1.38 MPa at 12 weeks. Young's

220   modulus was significantly lower in the OVX than in the control group at 2 and 4 weeks, but

221   the difference was no longer significant at 8 and 12 weeks (Figure 3D).

222

223   Figure 3. Mechanical properties of reattached supraspinatus tendons in ovariectomized and control

224   rats. (A) Ultimate load to failure (N). (B) Linear stiffness (N/mm). (C) Ultimate stress (MPa). (D)

225   Young's modulus (MPa).

226

227   **Histology**

228   HE staining of tendon-to-bone healing after cuff repair (Figure 4) shows fibrovascular tissue

229   at the tendon attachment site at 2 weeks. The trabecular bone and the fibrovascular tissue

230   were still immature in both the OVX and control groups at 4 weeks. At 8 weeks, some

231   chondroid cells appeared along with the trabecular bone and fibrovascular tissue in the

232   control group, but not in the OVX group. At 12 weeks, chondroid cells could be seen at the

233   tendon–bone interface in the control group, but in the OVX group, the fibrovascular tissue

234   was directly attached to bone without evidence of chondroid cells. No obvious differences

235   were seen in OVX and control tissues stained with safranin O at 2 and 4 weeks, but larger

236   areas of reddish-purple proteoglycan-stained chondroid tissue were seen in specimens from

237   control compared with OVX rats at 8 and 12 weeks (Figure 5). There were no obvious

238   differences in picrosirius red staining at 4 weeks, but at 8 and 12 weeks, it revealed better

239   collagen organization in tissue from control compared with OVX rats (Figure 6).

240

241   Figure 4. Hematoxylin and eosin (HE) staining of reattached supraspinatus tendons in

242   ovariectomized and control rats. (A) OVX, 2 weeks; (B) OVX, 4 weeks; (C) OVX, 8 weeks;

243   (D) OVX, 12 weeks; (E) control, 2 weeks; (F) control, 4 weeks; (G) control, 8 weeks; (H)

244   control 12 weeks.

245

Figure 5. Safranin O staining of reattached supraspinatus tendons in ovariectomized and control

mice. (A) OVX, 2 weeks; (B) OVX, 4 weeks; (C) OVX, 8 weeks; (D) OVX, 12 weeks; (E) control,

2 weeks; (F) control, 4 weeks; (G) control, 8 weeks; (H) control, 12 weeks.

249

Figure 6. Picrosirius red staining of reattached supraspinatus tendons in ovariectomized and control

rats. (A) OVX, 2 weeks; (B) OVX, 4 weeks; (C) OVX, 8 weeks; (D) OVX, 12 weeks; (E) control, 2

weeks; (F) control, 4 weeks; (G) control, 8 weeks; (H) control, 12 weeks.

253   The results of the cathepsin K assay of osteoclast at the tendon attachment and cancellous bone

254   sites are shown in Figure 7. The number of positively stained cells in cancellous bone was 17.33 ±

255   5.65 in the OVX group and 47.27 ± 26.33 in the control group at 2 weeks, 13.2 ± 10.2 and 29 ±

256   22.11 at 4 weeks, 11.47 ± 16.52 and 30.73 ± 17.05 at 8 weeks, and 3.53 ± 4.58 and 14 ± 14.99 at 12

257   weeks. The number of cathepsin K-positive cells at the insertion area were 23.2 ± 17.21 in the

258   control and 62.73 ± 29.27 in the OVX group at 2 weeks, 17.4 ± 12.05 and 53.6 ± 33.31 at 4 weeks,

259   12.27 ± 10.93 and 23 ± 13.05 at 8 weeks, and 11.8 ± 13.73 and 17.87 ± 14.95 at 12 weeks. The

260   number of cathepsin K-positive cells was significantly higher in the OVX than in the control groups

261   at 2, 4, 8, and 12 weeks at both the attachment site and in cancellous bone.

262

263   Figure 7. Immunostaining of cathepsin K of reattached supraspinatus tendons in ovariectomized and

264   control rats. (A) OVX, 2 weeks; (B) OVX, 4 weeks; (C) OVX, 8 weeks; (D) OVX, 12 weeks; (E)

265　control, 2 weeks; (F) control, 4 weeks; (G) control, 8 weeks; (H) control 12 weeks. (I) Number of

266　positive cells in cancellous bone and (J) number of positive cells in the insertion area.

267

268　**DISCUSSION**

269　In various animal models, agents that promote bone regeneration have been shown to accelerate

270　tendon-to-bone healing after rotator cuff repair.[1,10,12,13] However, those studies were conducted in

271　animals with normal BMD. Chen et al. reported that teriparatide increased humeral head bone

272　density improved the mechanical properties of the tendon enthesis in an ovariectomized rabbit

273　rotator cuff repair model but did not describe the characteristics of the enthesis after repair.[5] In this

274　study, at 2 and 4 weeks after surgery, biomechanical strength and development of matured

275　granulation tissue were reduced in the OVX group. At 8 and 12 weeks, the histology was quietly

276　different between 2 groups without significant reduction of the biomechanical properties. The

277　differences in the appearance of tendon reattachment were described as indirect insertion in the

278　OVX group, that is, without chondroid cells at the tendon–bone interface and direct insertion in the

279　control group, with the presence of chondroid cells. Thus, the results successfully demonstrated

280　biomechanical and histological alterations of tendon-to-bone healing after rotator cuff repair in

281　OVX rats.

282　　Biomechanical strength was significantly lower in the OVX group than in the control group at 2

283　and 4 weeks, with relatively mature granulation tissue at the repair site of control rats. The findings

284　suggest that immature granulation tissue interposed at the tendon–bone interface contributes to

285　biomechanical strength. An investigation of the effects of female sex steroids and calciotropic

286　hormones by Maman et al. reported that proliferation of tendon-derived cells was promoted by

287　commonly prescribed female sex and calciotropic hormones.[23] An *in vitro* study of the proliferation

288　and metabolism of tenocytes isolated from the Achilles tendons of ovariectomized, middle-aged,

289　and young rats by Torricelli et al. described the negative effects of aging and estrogen deficiency on

290　tendon metabolism and healing.[38] Endogenous estrogen has also been shown to promote healing of

291 the Achilles tendon in a rat model.[7] The effects of estrogen on tenocyte biosynthesis, apoptosis, and

292 tendon healing suggest that a deficiency induced by ovariectomy could result in the effects

293 described in the above studies.

294 The tissue histology findings at 8 and 12 weeks differed from those at 2 and 4 weeks, with

295 indirect insertion lacking chondroid cells in the OVX group and direct insertion including

296 chondroid cells in the control group. Areas of positive safranin O staining were larger in the control

297 group than in the OVX group at 8 and 12 weeks. This plus the finding of increased cathepsin K

298 expression in OVX rats suggests that activated osteoclast may have been involved in the formation

299 of indirect insertions. The histological differences did not affect the biomechanical properties of the

300 two groups at 8 and 12 weeks. The cellular structure and distribution of tendon–bone interface at 12

301 weeks after rotator cuff repair resembled a normal tendon insertion. However, a study of the three-

302 dimensional ultrastructure found morphological differences at repaired, compared with normal,

303 undisturbed tendon insertion sites that might result in qualitative and/or quantitative differences.[19] A

304 recent systematic review of studies of healing and repair in injured and degenerated supraspinatus

305 enthesis found that the original graded transitional tissue of the fibrocartilaginous insertion was not

306 recreated after the tendon was surgically reattached to bone. Following reattachment, the enthesis

307 may not regain mechanical strength comparable with that of the native enthesis.[18] It is well known

308 that following anterior cruciate ligament (ACL) reconstruction, the interface at the graft tendon–

309 bone tunnel develops an indirect insertion, even though the postoperative outcome is generally

310 clinically acceptable.[4,27,34] The information available from previous studies may be of help in

311 accounting for the lack of significant biomechanical differences of indirect and direct insertions.[31]

312 The bone quality of the proximal humerus should be evaluated prior to rotator cuff repair using

313 suture anchors. The presence of low BMD can result in retear of the repaired rotator cuff, and the

314 BMD of the symptomatic shoulder can be lower than that in the asymptomatic contralateral

315 shoulder.[18] Aside from female gender, no other clinical variables present as high risk of

316 osteoporosis.[29]

317   Some limitations should be kept in mind when interpreting the present findings. First, acutely

318   created tear and immediate repair do not reflect chronic degenerative rotator tears. Consequently,

319   the findings in this rat model may not directly apply to humans because the healing processes in

320   healthy animals may not mirror those that are obtained in clinical practice. However, given the

321   anatomic similarities of humans and rats, this model has been widely used to investigate the healing

322   mechanism and methods of healing enhancement. Second, the biomechanical and histological

323   evaluation ended 12 weeks after surgery and may have missed additional subsequent events.

324   Especially, the biomechanical findings were significant only during the early timepoints; the study

325   may have been underpowered to detect residual differences at the later points. Third, there was not

326   control present to limit any additional variables present in the ovariectomized state, such as

327   endocrine or hormonal controls, that could have impacted the differences in tendon to bone healing

328   response noted at 8 and 12 weeks. Fourth, given the large effect size, the sample was relatively

329   small and may have been underpowered to detect some significant differences. The strengths of this

330   study include a clear demonstration of morphological and biomechanical differences in

331   ovariectomized and nonovariectomized rats in a rotator cuff Repair model.

332   In conclusion, an estrogen-deficient state due to ovariectomy, rather than low BMD, leading to

333   low decreased biomechanical strength and poor chondroid tissue formation following rotator cuff

334   repair.

335

336   **References**

337

338   1. Aydin A, Kenar H, Atmaca H, et al. The short- and long- term effects of estrogen deficiency on

339   apoptosis in musculoskeletal tissues: an experimental animal model study. *Arch Iran Med.*

340   2013;16(5):271-276.

341   2. Benjamin M, Evans EJ, Copp L. The histology of tendon attachments to bone in man. *J

342   Anat.*1986;149(12):89-100.

343   3. Boileau P, Brassart N, Watkinson DJ, et al. Arthroscopic repair of full-thickness tears of the

344   supraspinatus: does the tendon really heal? *J Bone Joint Surg Am.* 2005;87(6):1229-1240.

345   4. Chen CH. Strategies to enhance tendon graft--bone healing in anterior cruciate ligament

346   reconstruction. *Chang Gung Med J.* 2009;32(5):483-493.

347   5. Chen X, Giambini H, Ben-Abraham E, et al. Effect of Bone Mineral Density on Rotator

348   Cuff Tear: An Osteoporotic Rabbit Model. *PLoS One.* 2015;10(10):e0139384.

349   6. Chung SW, Oh JH, Gong HS, et al. Factors affecting rotator cuff healing after arthroscopic

350   repair: osteoporosis as one of the independent risk factors. *Am J Sports Med.*

351   2011;39(10):2099-2107.

352   7. Circi E, Akpinar S, Balcik C, et al. Biomechanical and histological comparison of the

353   influence of oestrogen deficient state on tendon healing potential in rats. *Int Orthop.*

354   2009;33(5):1461-1466.

355   8. Cooper RR, Misol S. Tendon and ligament insertion. A light and electron microscopic

356   study. *J Bone Joint Surg Am.* 1970;52(1):1-20.

357   9. Franceschi F, Ruzzini L, Longo UG, et al. Equivalent clinical results of arthroscopic

358   single-row and double-row suture anchor repair for rotator cuff tears: a randomized

359   controlled trial. *Am J Sports Med.* 2007;35(88):1254-1260.

360   10. Galatz LM, Gerstenfeld L, Heber-Katz E, et al. Tendon regeneration and scar formation:

361   The concept of scarless healing. *J Orthop Res.* 2015;33(6):823-831.

362   11. Goutallier D, Postel JM, Gleyze P, et al. Influence of cuff muscle fatty degeneration on

363   anatomic and functional outcomes after simple suture of full-thickness tears. *J Shoulder

364   Elbow Surg.*2003;12(6):550-554.

365   12. Gulotta LV, Kovacevic D, Ehteshami JR, et al. Application of bone marrow-derived

366   mesenchymal stem cells in a rotator cuff repair model. *Am J Sports Med.*

367   2009;37(11):2126-2133.

368   13. Gulotta LV, Kovacevic D, Packer JD, et al. Bone marrow-derived mesenchymal stem cells

369   transduced with scleraxis improve rotator cuff healing in a rat model. *Am J Sports Med.*

370   2011;39(6):1282-1289.

371   14. Hettrich CM, Beamer BS, Bedi A, et al. The effect of rhPTH on the healing of tendon to bone in

372   a rat model. *J Orthop Res.* 2011;30(5):769-774.

373   15. Hettrich CM, Gasinu S, Beamer BS, et al. The effect of mechanical load on tendon-to-bone

374   healing in a rat model. *Am J Sports Med.* 2014;42(5):1233-1241.

375   16. Holoz L, Hapa O, Barber FA, et al. Suture Anchor Fixation in Osteoporotic Bone: A

376   Biomechanical Study in an Ovine Model. *Arthroscopy.* 2017;33(1):68-74.

377   17. Honda H, Gotoh M, Kanazawa T, et al. Effects of lidocaine on torn rotator cuff tendons. *J

378   Orthop Res.* 2016;34(9):1620-1627.

379   18. Jensen PT, Lambertsen KL, Frich LH. Assembly, maturation, and degradation of the

380   supraspinatus enthesis *J Shoulder Elbow Surg*.2018;27(4):739-75.

381   19. Kanazawa T, Gotoh M, Ohta K, et al. Histomorphometric and ultrastructural analysis of the

382   tendon-bone interface after rotator cuff repair in a rat model. *Sci Rep.* 2016;20(6):33800.

383   20. Kanazawa T, Gotoh M, Ohta K, et al. Novel characteristics of normal supraspinatus insertion in

384   rats: an ultrastructural analysis using three-dimensional reconstruction using focused ion

385   beam/scanning electron microscope tomography. *Muscles Ligaments Tendons J.* 2014;4(2):182-187.

386   21. Kanazawa T, Gotoh M, Ohta K, et al. Three-dimensional ultrastructural analysis of

387   development at the supraspinatus insertion by using focused ion beam/scanning electron

388   microscope tomography in rats. *J Orthop Res.* 2016;34(6):969-976.

389   22. Lu HH, Thomopoulos S. Functional attachment of soft tissues to bone: development, healing,

390   and tissue engineering. *Annu Rev Biomed Eng.* 2013;15:201-226.

391   23. Maman E, Somjen D, Maman E, et al. The response of cells derived from the supraspinatus

392   tendon to estrogen and calciotropic hormone stimulations: in vitro study. *Connet Tissue Res.*

393   2016;57(2):124-130.

394 24. Martinek V, Latterman C, Usas A, et al. Enhancement of tendon-bone integration of anterior

395 cruciate ligament grafts with bone morphogenetic protein-2 gene transfer: a histological and

396 biomechanical study. *J Bone Joint Surg Am.* 2002;84-A(7):1123-1131.

397 25. Mattia L, Umile GL, Giuseppe N, et al. Histopathological Scores for Tissue-Engineered,

398 Repaired and Degenerated Tendon: A Systematic Review of the Literature. *Curr Stem Cell Res*

399 *Ther.* 2015;10(1):43-55.

400 26. Messner K. Postnatal development of the cruciate ligament insertions in the rat knee.

401 morphological evaluation and immunohistochemical study of collagens types I and II. *Acta*

402 *Anat.*1997;160(4):261-268.

403 27. Moulton SG, Steineman BD, Donahue TL, Fontboté CA, Cram TR, LaPrade RF. Direct versus

404 indirect ACL femoral attachment fibres and their implications on ACL graft placement. *Knee Surg*

405 *Sports Traumatol Arthrosc.* 2017;25(1):165-171.

406 28. Nakamura H, Gotoh M, Kanazawa T, et al. Effects of corticosteroids and hyaluronic acid on

407 torn rotator cuff tendons in vitro and in rats. *J Orthop Res.* 2015;33(10):1523-1530.

408 29. Oh JH, et al. The measurement of bone mineral density of bilateral proximal humeri using DXA

409 in patients with unilateral rotator cuff tear. *Osteoporos   Int.* 2014;25(11):2639-2648.

410 30. Oh JH, Song BW, Lee YS. Measurement of volumetric bone mineral density in proximal

411 humerus using quantitative computed tomography in patients with unilateral rotator cuff tear. *J*

412 *Shoulder Elbow Surg.* 2014;23(7):993-1002.

413 31. Robert H, Es-Sayeh J, Heymann D, et al. Hamstring insertion site healing after anterior cruciate

414 ligament reconstruction in patients with symptomatic hardware or repeat rupture: a histologic study

415 in 12 patients. *Arthroscopy.* 2003;19(9):948-954.

416 32. Rodeo SA, Arnoczky SP, Torzilli PA, et al. Tendon-healing in a bone tunnel. A biomechanical

417 and histological study in the dog. *J Bone Joint   Surg Am.*1993;75(12):1795-1803.

418 33. Rodeo SA. Use of Recombinant Human Bone Morphogenic Protein-2 to Enhance Tendon

419 Healing in a Bone Tunnel. *Am J Sports Med.* 1999;27(4):476-488.

420   34. Sasaki N, Ishibashi Y, Tsuda E, et al. The femoral insertion of the anterior cruciate ligament:

421   discrepancy between macroscopic and histological observations. *Arthroscopy.*

422   2012;28(8):1135-1146.

423   35. Soslowsky LJ, Carpenter JE, DeBano CM, et al. Development and use of an animal model for

424   investigations on rotator cuff disease. *J Shoulder Elbow Surg.* 1996;5(5):383-392.

425   36. Sugaya H, Maeda K, Matsuki K, et al. Repair integrity and functional outcome after

426   arthroscopic double-row rotator cuff repair: a prospective outcome study. *J Bone Joint Surg Am.*

427   2007;89(5):953-960.

428   37. Tabuchi K, Soejima T, Kanazawa T, et al. Chronological changes in the collagen-type

429   composition at tendon-bone interface in rabbits. *Bone Joint Res.* 2012;1(9):218-224.

430   38. Torricelli P, Veronesi F, Pagani S, et al. In vitro tenocyte metabolism in aging and oestrogen

431   deficiency. *Age (Dordr).* 2013;35(6):2125-2136.

432   39. Zumstein MA, Jost B, Hempel J, et al. The clinical and structural long-term results of open

433   repair of massive tears of the rotator cuff. *J Bone Joint Surg Am.* 2008;90(11):2423-2431